SUPPLEMENTARY INFORMATION

Design and evaluation of BOOGIE: a collector for the analysis of cloud composition and processes: Biological, Organics, Oxidants, soluble Gases, inorganic Ions and metal Elements

Mickael Vaitilingom[1,2*], Christophe Bernard[3], Mickaël Ribeiro[1,3], Christophe Berthod[4], Angelica Bianco[1], Laurent Deguillaume[1,3*]

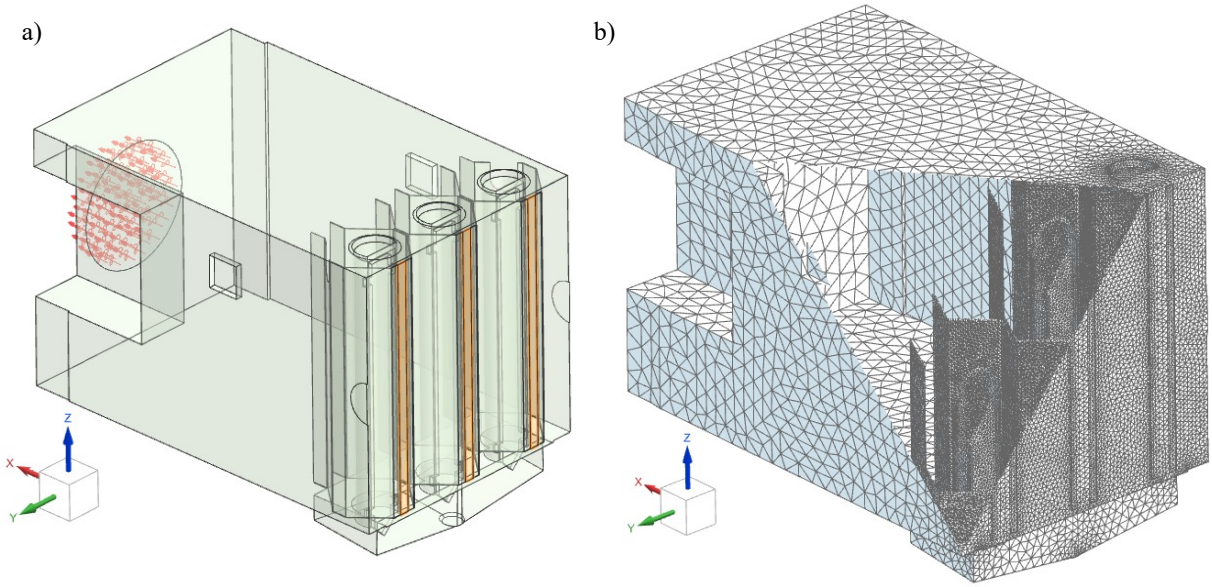

Figure S1. a) Fluid domain corresponding to the air volume inside the collector (translucency display). The three orange zones are the air inlet faces, and the red arrows represent the outlet corresponding to the action of the fan. b) View section of the finite element model (internal elements are dismissed, element edges are displayed on the faces only).

Table S1. Size and mass of each class of aqueous particles used for the CFD simulation.

Class	Diameter (µm)	Mass (g)
1	5	$6.54\ 10^{-11}$
2	6	$1.13\ 10^{-10}$
3	7	$1.79\ 10^{-10}$
4	8	$2.68\ 10^{-10}$
5	9	$3.82\ 10^{-10}$
6	10	$5.24\ 10^{-10}$
7	15	$1.77\ 10^{-9}$
8	20	$4.19\ 10^{-9}$

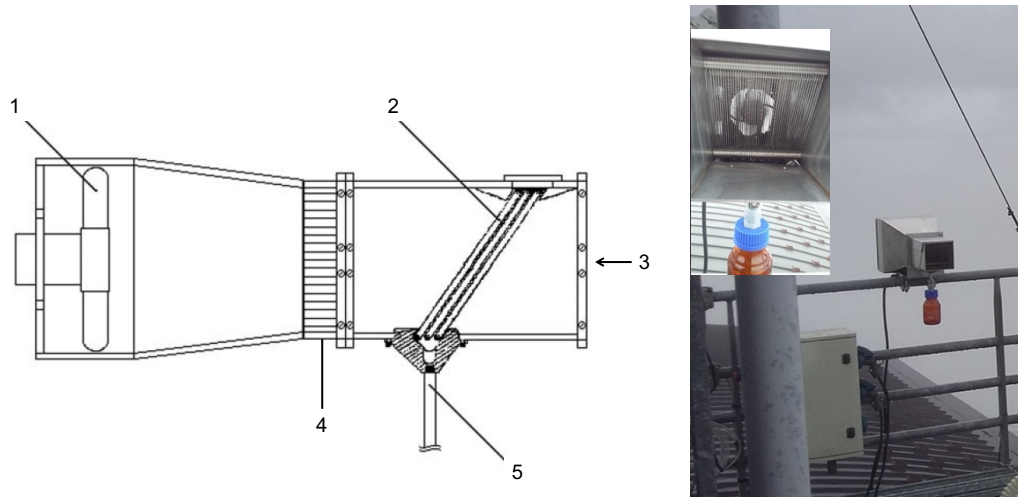

Figure S2. Left: Construction of the CASCC2 sampler: 1 = ventilator fan; 2 = strands; 3 = inlet; 4 = flow straightener; 5 = sample drainage. Right: CASCC2 installed at PUY. Picture : M. Vaitilingom.

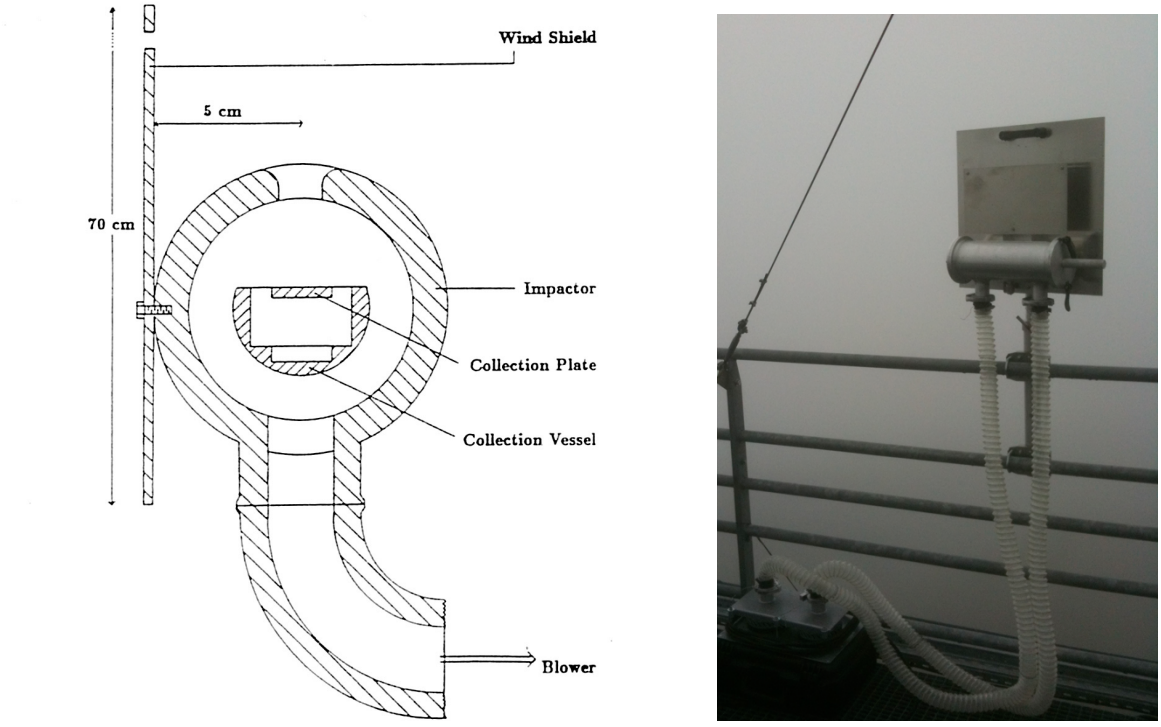

Figure S3. Cross section of the CWS (left) and the CWS installed at PUY (right). Picture : M. Vaitilingom.

Description of the chemical and biological analysis

Immediately after collection, the samples were fixed and frozen in appropriate vessels at the PUY station. The collectors were cleaned using ultrapure water and sterilised by an autoclave (121 °C, 20 min), before sampling; sterile ultrapure water was sprayed on the collector and these waters flowing into the collector inlet and vessel were collected as blank samples and analysed as the cloud water samples. Considering the chemical and microbial targets listed above, all analysis given measurements under the limit of detection.

The main ions (Cl^-, NO_3^-, NH_4^+, SO_4^{2-}, Na^+, Ca^+, Mg^+, K^+) were analysed using ion chromatography. The instruments used were a Dionex DX320 for anions (column AS11, eluent KOH) and Dionex ICS1500 for cations (column CS16, eluent hydroxymethanesulfonate acid). The accuracy of the ion chromatographic analysis was 10%.

The formaldehyde concentration was measured using a miniaturised fluorometric assay (Li et al., 2007). The reaction medium comprised 60 µL of ammonium acetate solution AAA (0.2 M in ethanol solution 50% v/v), 60 µL of ethanol (96°), and 120 µL of cloud water sample. This solution was mixed and incubated in a 96-well black flat-bottomed plate 25 min before reading (λex = 375 nm and λem = 490 nm) on a TECAN spectrofluorometer. The uncertainty of measurement was <5%, and the detection limit (DL) was 0.1 µM; duplicate measurements were performed or triplicate if the standard deviation was over 5%.

The hydrogen peroxide concentration was measured using an enzymatic fluorometric assay involving horse radish peroxidase (HRP) and 4-Hydroxyphenylacetic acid (HPAA), producing a fluorescent dimeric compound with hydrogen peroxide. After sampling, 10 and 50 µL of cloud water sample were mixed on site with 200 µL of reagent solution (HRP + HPAA) in triplicate and incubated at room temperature (>17 °C) 5 min before freezing at -25 °C until analysis. The measurement was performed using fluorimetry (λex = 320 nm and λem = 390 nm). Analyses were performed in duplicate or triplicate if the standard deviation of measurement exceeded 5%, the DL was of 0.07 µM (Vaïtilingom et al., 2013).

ATP and ADP concentrations were measured in cloud water samples using the ATP Biomass Kit HS (Biothema©) and a Biolumineter (Lumac Biocounter M2500). The cloud water samples (0.2 mL) were strongly mixed in a sterile microtube with an equal volume of extractant B/S from the ATP Biomass Kit HS (Biothema©); this mixture was used for ATP determination and frozen until analysis. ATP concentrations were determined by bioluminescence (Lazrus et al., 1985) using a Biolumineter (Lumac Biocounter M2500). ADP concentrations were determined after the direct transformation of ADP to ATP in a luminometer tube in the presence of pyruvate kinase and phosphoenolpyruvate (Koutny et al., 2006; Vaïtilingom et al., 2013). A small volume of the mixture (sample + extractant B/S: 60 µL) was used to determine the ATP or ADP concentrations in triplicate; the standard deviations of the measurements were <5%.

Note: All bio-physico-chemical data of this study are available as all cloud data since 2001 on the PUYCLOUD database (https://www.opgc.fr/data-center/public/data/puycloud).

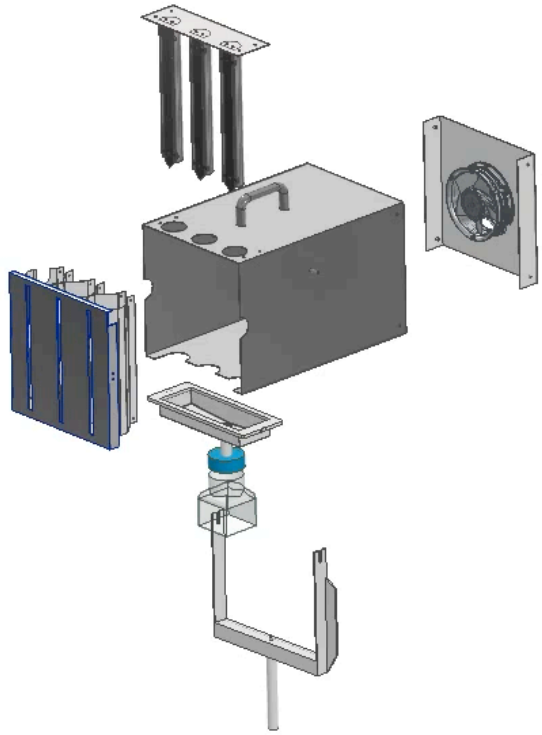

Movie 1. Collector installation procedure at the sampling site. See file “Sampler-assembly.mp4”.

Figure S4. 3 BOOGIE cloud water collectors deployed at PUY during a field campaign. Picture : L. Deguillaume.

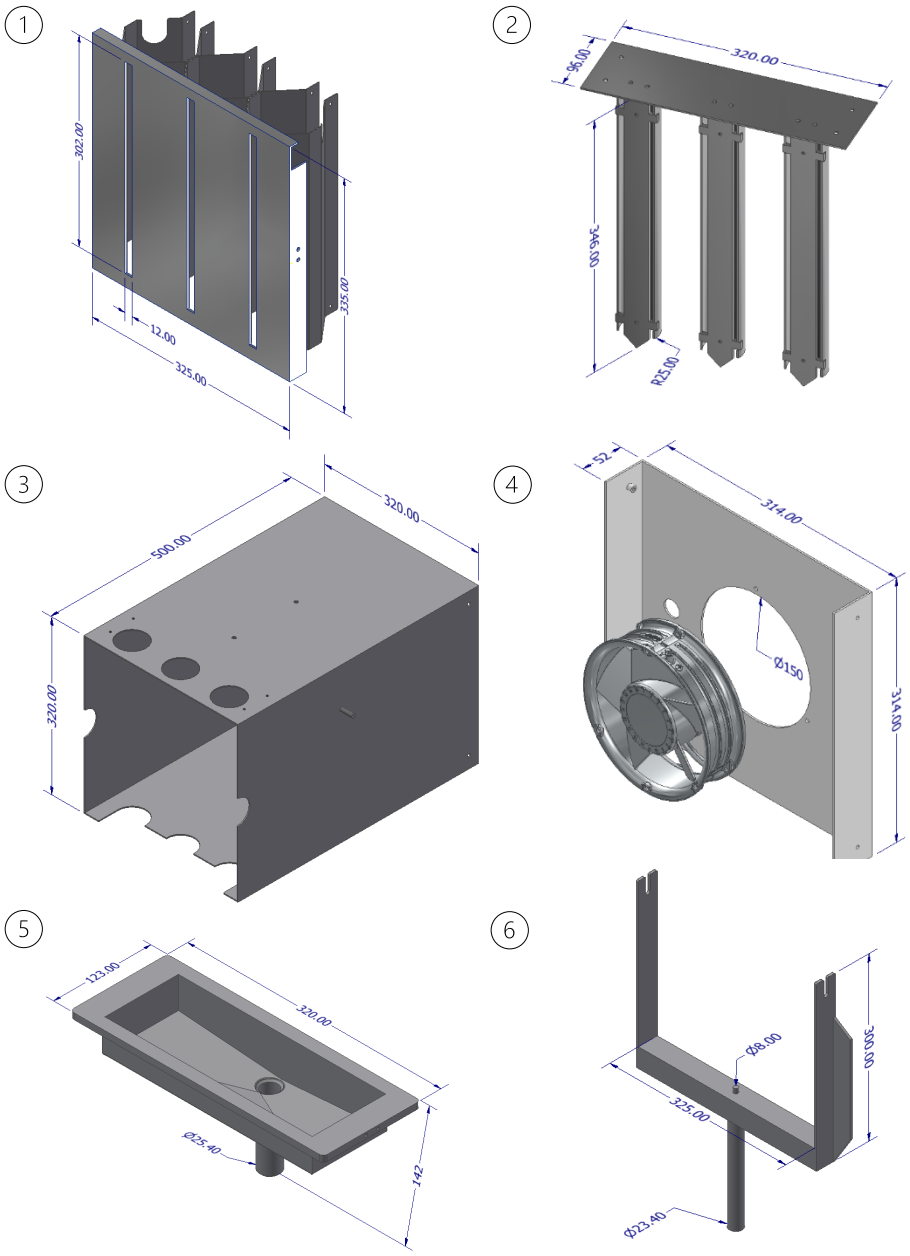

Figure S5. Parts of the cloud sampler with the size dimension: (1) front face with the three slots; (2) impaction plates; (3) collector body; (4) rear face with the fan; (5) funnel; (6) instrument holder.

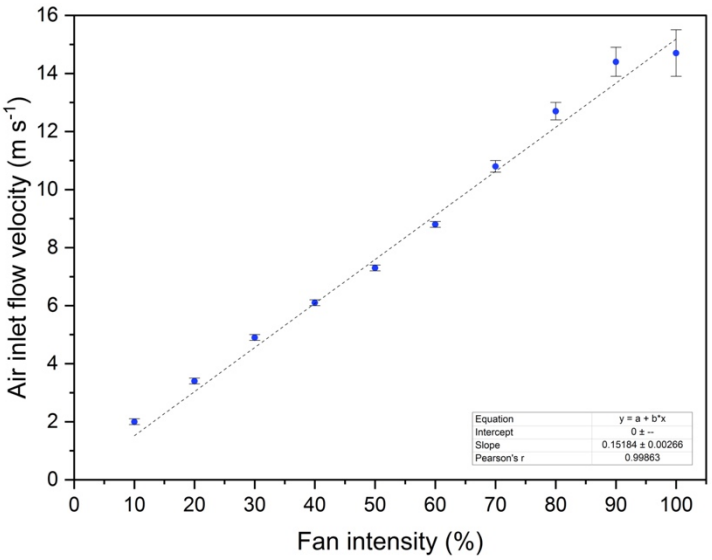

Figure S6. Measured air inlet flow velocity depending on the fan intensity. Standard deviations have been calculated based on nine measurements: velocities have been quantified on the three slots at different heights (top, mid-height, bottom).

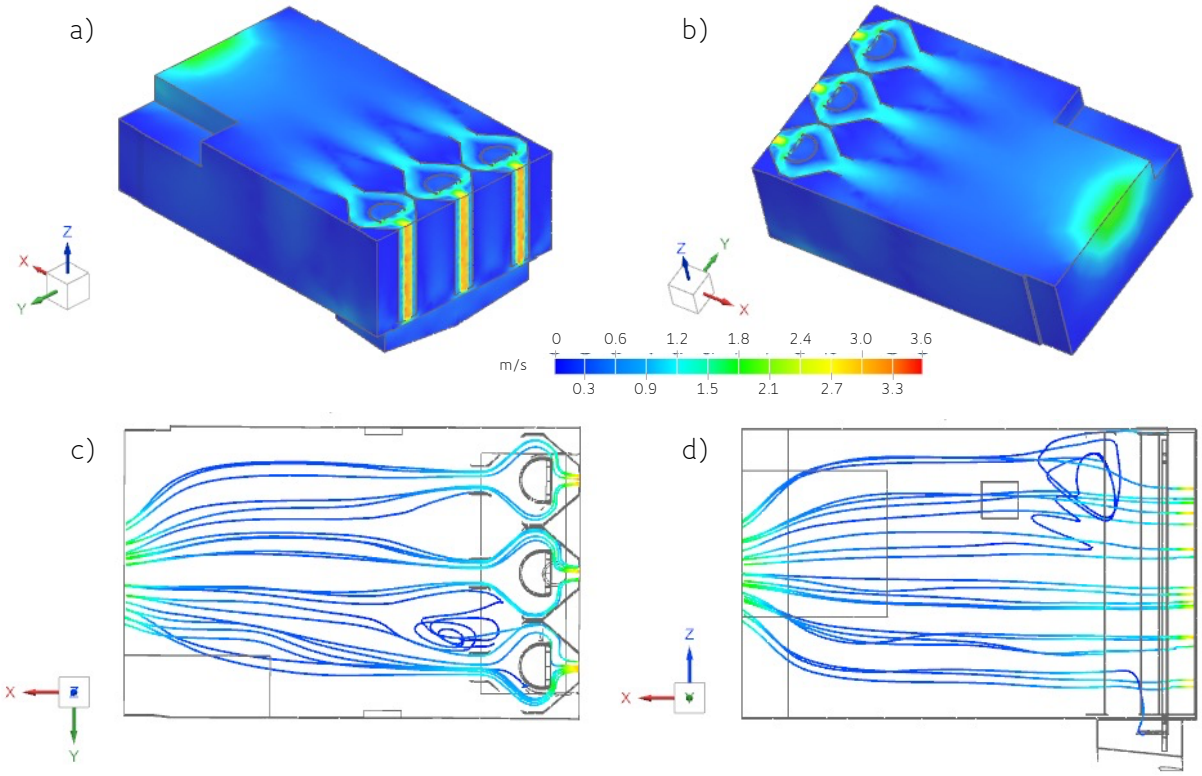

Figure S7. a) and b) Cutting plane in the flow velocity contour (in magnitude) in the case of a 2 m s^{-1} air outlet flow velocity; c) and d) set of streamlines in the collector (c- right view, d - top view) in the case of a 2 m s^{-1} air outlet flow velocity. Colour code indicates the different air velocities inside the collector.

		Class of particle							
Outlet velocity ($m\ s^{-1}$)	Injected number	1	2	3	4	5	6	7	8
1	59725	17952	17984	17956	17966	17983	17974	18541	20297
2	59725	18616	18634	18632	18653	18776	18979	21415	26258
3	59725	18844	18878	18992	19187	19547	20014	24560	32715
4	59725	19009	19106	19351	19771	20365	21210	27962	39686
5	59725	19162	19334	19765	20396	21303	22421	31528	46504
6	59725	19277	19581	20189	21100	22304	23733	35221	53139
7	59725	19426	19900	20699	21864	23334	25123	38975	57423
8	59725	19568	20208	21221	22682	24443	26562	42555	58267
9	59725	19743	20535	21798	23446	25533	27971	46245	58318
10	59725	19945	20922	22409	24302	26689	29423	49821	58372

Table S2. Particle impact tracking: number of droplets that impact the collection plates depending on the outlet velocity and the class of particles.

Date of sampling	Tstart (UTC)	Duration (min)	Mean Temperature (°C)	Standard Dev. Temp. (°C)	Wind speed ($m\ s^{-1}$)	Standard Dev. Wind speed ($m\ s^{-1}$)	Mean LWC_{meas} ($g\ m^{-3}$)	Standard Dev. Mean LWC_{meas} ($g\ m^{-3}$)	R_{eff} (µm)	Standard Dev. R_{eff} (µm)	Collected water mass (g)
03/05/2016	6h55	60	3.00	0.19	3.01	0.75	0.31	0.02	8.12	0.43	89.50
01/06/2016	12h50	90	6.35	0.24	8.11	0.51	0.15	0.01	10.76	0.68	59.00
04/06/2016	18h45	180	7.76	0.24	0.26	0.12	0.31	0.06	6.59	0.62	326.00
28/06/2016	6h45	60	9.30	0.14	2.27	0.44	0.35	0.13	4.63	0.97	105.00
02/07/2016	00h00	360	9.67	1.00	12.02	1.49	0.26	0.05	6.07	0.67	440.00
05/04/2018	7h25	115	-0.33	0.19	ND	ND	0.20	0.08	9.85	2.12	100.00
03/05/2018	7h30	130	2.22	0.32	ND	ND	0.23	0.06	6.58	0.86	150.00
09/05/2018	8h05	125	7.54	0.50	ND	ND	0.49	0.16	9.07	1.72	300.00
13/06/2018	8h25	60	5.90	0.12	ND	ND	0.21	0.06	5.64	0.46	50.00
08/10/2018	11h15	210	7.76	0.12	7.00	0.98	0.34	0.16	5.50	2.03	380.00
16/07/2021	8h40	180	9.90	0.25	2.20	0.43	0.71	0.09	10.10	1.22	684.00
08/10/2021/S1	6h40	150	1.90	0.06	9.20	0.71	0.56	0.04	10.70	0.29	485.00
08/10/2021/S2	6h40	150	1.90	0.06	9.20	0.71	0.56	0.04	10.70	0.29	461.00
13/10/2021/S1	6h30	190	2.90	0.20	2.70	0.70	0.28	0.09	9.50	1.05	280.00
13/10/2021/S2	6h30	190	2.90	0.20	2.70	0.70	0.28	0.09	9.50	1.05	259.00
26/10/2021/S1	8h40	65	4.80	0.09	4.40	0.93	0.21	0.09	10.70	3.48	67.00
26/10/2021/S2	8h40	65	4.80	0.09	4.40	0.93	0.21	0.09	10.70	3.48	60.00
30/03/2022	8h35	50	3.28	0.19	ND	ND	0.37	0.17	10.09	1.28	98.00
25/04/2022	7h25	195	2.31	0.38	11.05	1.25	0.42	0.15	9.87	1.08	377.00
11/01/2023	7h30	120	2.23	0.13	ND	ND	0.48	0.03	11.06	0.30	310.00

Table S3. Cloud sampling characteristics: Date/duration, and average data over the sampling duration: meteorological parameters (T, wind speed), microphysical parameters (liquid water content [LWC], effective radius) and mass of the collected cloud water. For clouds on 8/10/2021, 13/10/21, and 26/10/2021, two BOOGIE samplers were deployed in parallel. ND: Not Determined.

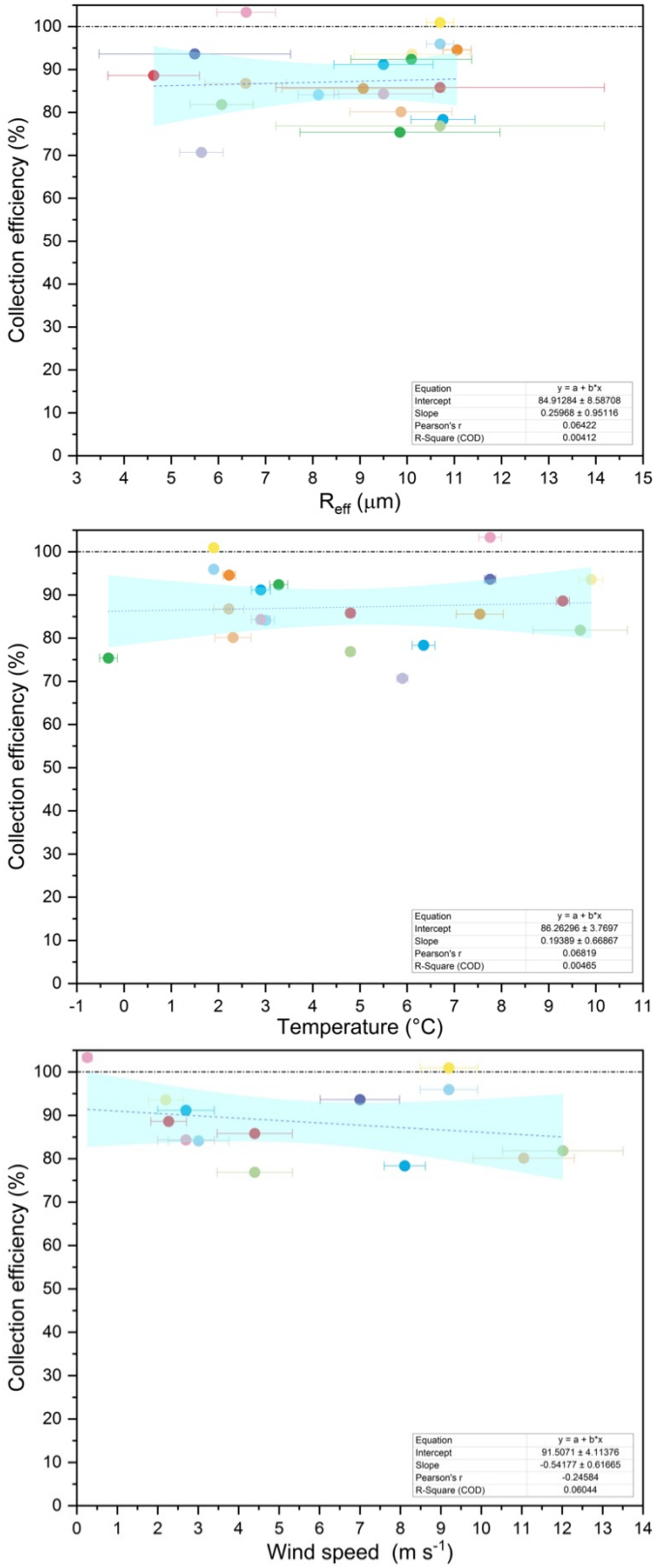

Figure S8. Collection efficiency of the BOOGIE collector of the cloud samples (coloured dots) vs meteorological and microphysical parameters (effective radius, temperature, wind speed). Error bars correspond to the standard deviation. The dotted blue line represents the linear fit of the experimental data, and the blue area denotes the 95% confidence interval of this fit.

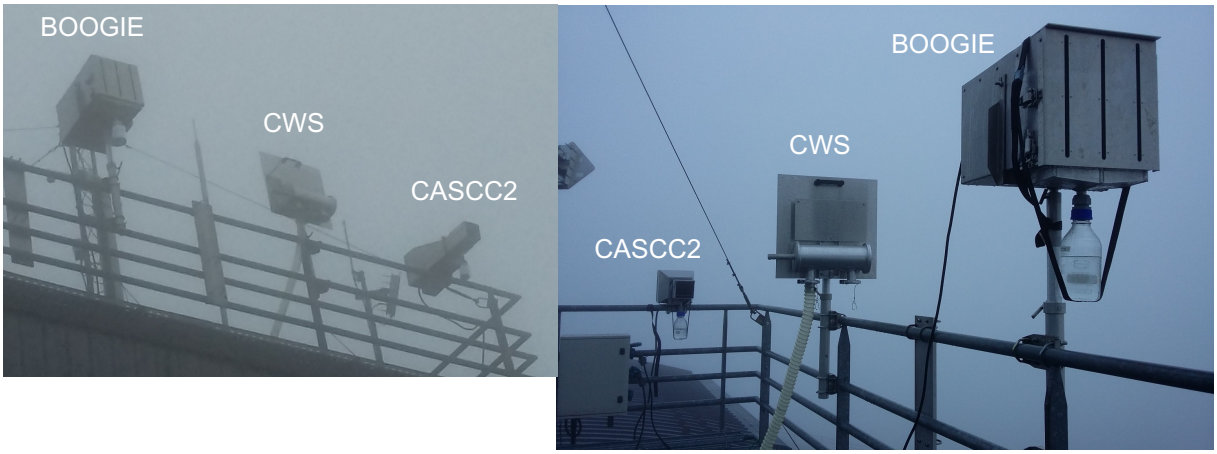

Figure S9. Inter-comparison experiment under cloudy conditions at the PUY station, from left to right: the BOOGIE, CWS, and CASCC2 samplers. Picture : M. Vaitilingom.

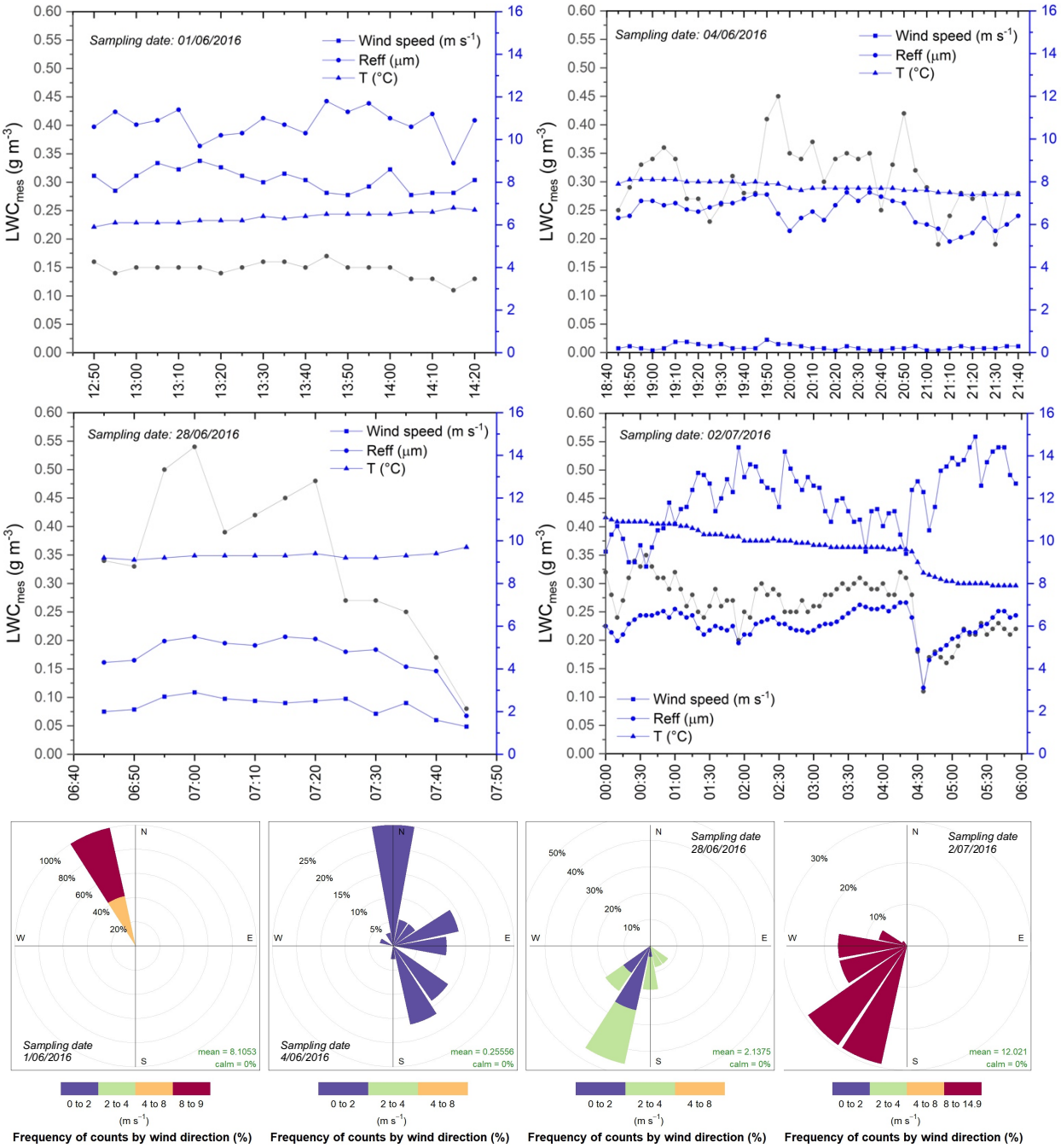

Figure S10. Above: Time evolution of meteorological and microphysical parameters of the four cloud events sampled during the inter-comparison experiment of cloud samplers at PUY in 2016. Below: Illustration of the distribution of wind direction and speed during the sampling period ("calm" corresponds to values <0.5 m s^{-1}). Colours indicate wind speed ranges associated with each direction.

a)

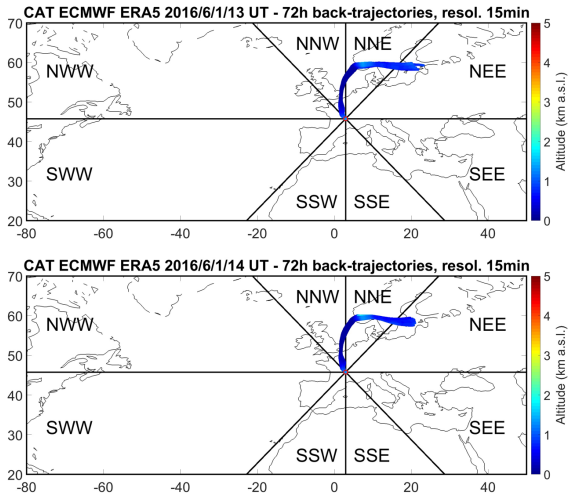

Sampling period: 01/06/2016 – UT: 13:00 & 14:00

b)

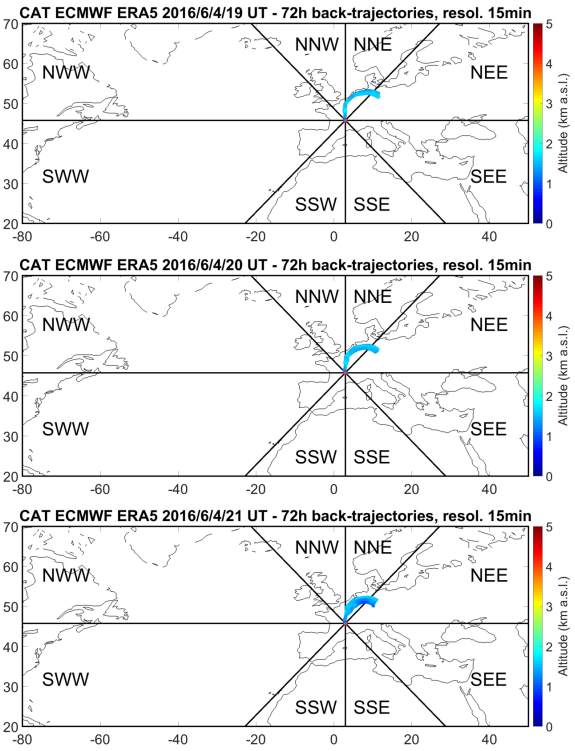

Sampling period: 04/06/2016 – UT: 19:00 & 20:00 & 21:00

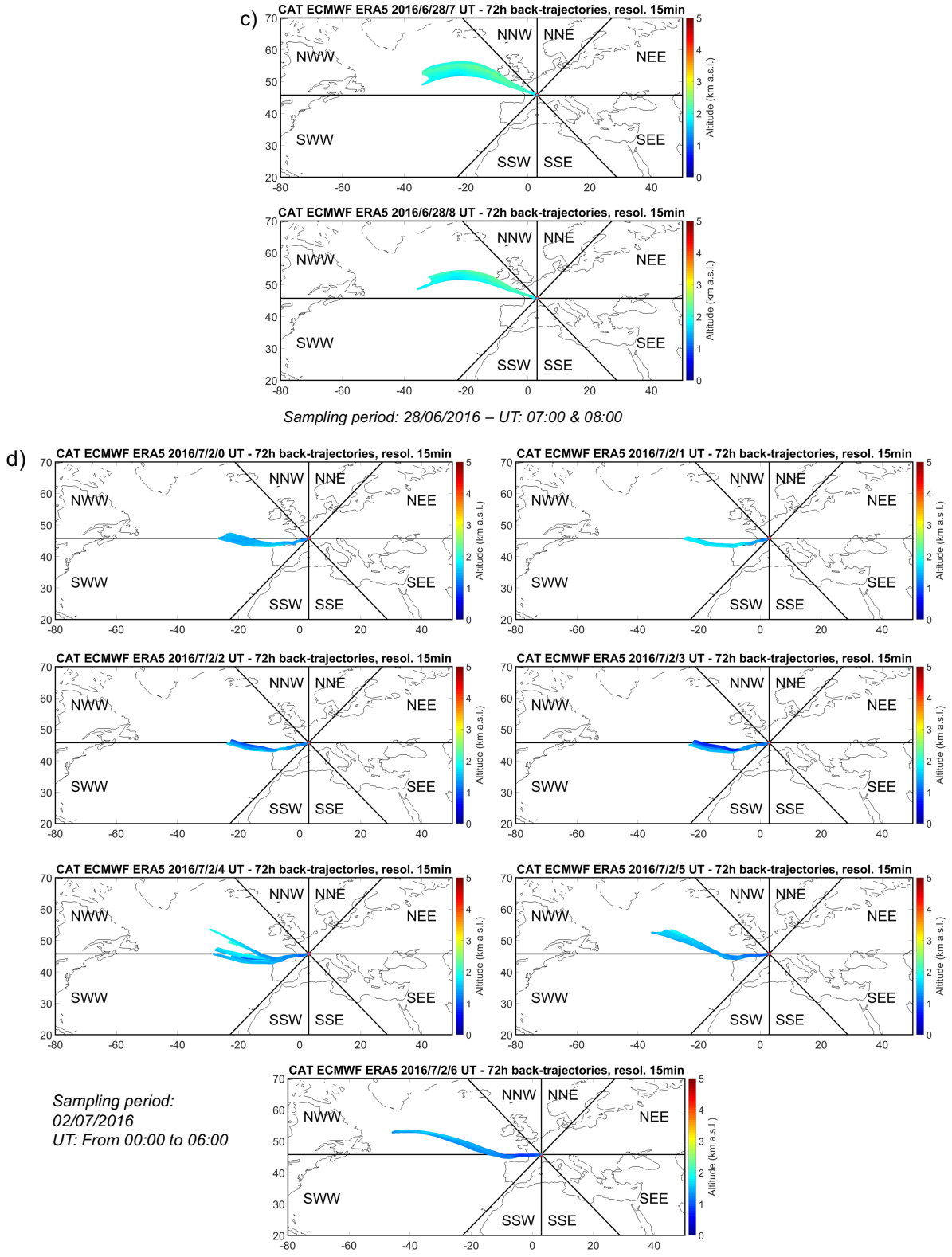

Figure S11. Seventy-two-hour back-trajectory plots of the four cloud events sampled in 2016 calculated using the CAT model. Set of 45 back trajectories were calculated every hour in volume +/− 0.1° in latitude and longitude. The colour code corresponds to the altitude of the air mass above sea level (a.s.l.).

Note. The temporal resolution was 15 min, and the total duration was 72 h. The vertical starting altitude of the back trajectories was deduced from the pressure measured at the PUY summit, considering hydrostatic equilibrium. Trajectories were calculated between the summit and 50 m below it (corresponding to 4 hPa) to consider the ascent of air masses arriving below the observatory from the slopes of the PUY.

	Date	Na^+	Cl^-	NH_4^+	SO_4^{2-}	NO_3^-	Mg^{2+}	K^+	Ca^{2+}
BOOGIE	04/06/2016	7.3	4.4	131.8	23.0	73.8	2.4	3.1	15.7
CASCC2	04/06/2016	5.4	7.1	174.1	32.9	124.5	14.7	2.7	45.6
CWS	28/06/2016	28.1	13.5	188.5	23.7	56.8	2.7	4.4	18.6
BOOGIE	28/06/2016	20.5	12.3	154.4	15.2	44.9	4.0	3.7	16.9
CASCC2	28/06/2016	23.1	13.2	222.7	24.3	46.8	4.6	8.3	17.6
CWS	02/07/2016	15.7	9.9	170.2	40.9	38.7	2.3	2.0	21.4
BOOGIE	02/07/2016	18.8	10.6	163.5	39.3	40.2	3.6	2.7	34.1
CASCC2	02/07/2016	15.7	10.7	211.8	45.4	42.2	4.6	2.7	22.6

Table S4. Chemical analysis of 4 cloud events: aqueous concentrations of main inorganic ions in µmol L^{-1}.

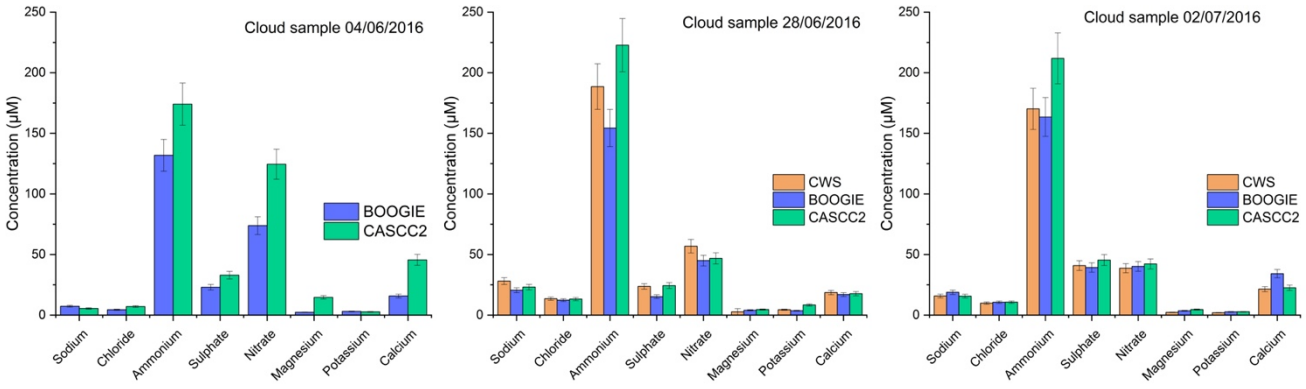

Figure S12. Histograms presenting the concentrations of anions and cations for the three cloud samples collected using CWS, BOOGIE, and CASCC2 in parallel. The error bars correspond to a 10% instrument uncertainty.

Note: Following the study by Renard et al. (2020) on cloud samples collected at PUY, the three cloud events presented below were classified according to their chemical properties (*i.e.*, inorganic ion concentrations). The three events were classified as "continental" because they present significant NH_4^+, SO_4^{2-}, and NO_3^- concentrations, indicating that they were influenced by emission from the continental surface.

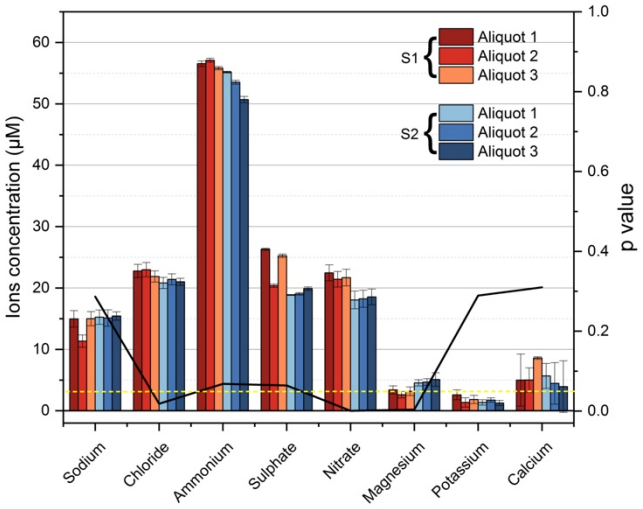

Figure S13. Histograms presenting the concentrations for a specific cloud sampled on 08/07/2021 at PUY with two BOOGIE collectors. This time, three aliquots were analysed twice (error bars) using ion chromatography. p-values are indicated with the black line and the yellow dashed line indicates the threshold of p = 0.05.

08/07/2021		Na^+	Std	Cl^-	Std	NH_4^+	Std	SO_4^{2-}	Std	NO_3^-	Std	Mg^{2+}	Std	K^+	Std	Ca^{2+}	Std
S1	Aliq. 1	14.9	1.3	22.8	1.1	56.5	0.4	26.3	0.2	22.5	1.3	3.4	0.6	2.6	0.8	5.0	4.2
	Aliq. 2	11.3	1.0	23.0	1.2	57.1	0.3	20.4	0.3	21.4	1.3	2.6	0.5	1.3	0.8	5.0	2.0
	Aliq. 3	15.0	1.1	21.9	0.9	55.8	0.3	25.2	0.3	21.7	1.3	3.2	0.7	1.8	0.6	8.6	0.2
S2	Aliq. 1	15.2	1.2	20.8	0.9	55.2	0.1	18.9	0.1	18.0	1.4	4.5	0.5	1.3	0.4	5.7	2.0
	Aliq.2	15.1	1.3	21.4	0.9	53.5	0.3	19.0	0.2	18.2	1.4	4.7	0.5	1.7	0.3	4.5	3.4
	Aliq. 3	15.4	0.7	21.0	0.6	50.7	0.5	19.9	0.3	18.5	1.3	5.1	1.1	1.3	0.4	3.9	4.2

Table S5. Chemical analysis of cloud events 08/07/2021: aqueous concentrations of main inorganic ions in µmol L^{-1}; aliquots were analysed twice – standard deviations are indicated in the table (Std).

	01/06/2016	04/06/2016	28/06/2016	02/07/2016
CWS	0.3	0.3	0.3	0.3
BOOGIE	0.3	0.3	0.2	0.3
CASCC2	0.3	0.3	0.3	0.3

Table S6. ATP/ADP ratios from the cloud microbiota collected by the three different samplers over four cloud events.

References

Koutny, M., Sancelme, M., Dabin, C., Pichon, N., Delort, A.-M., and Lemaire, J.: Acquired biodegradability of polyethylenes containing pro-oxidant additives, Polymer Degradation and Stability, 91, 1495-1503, https://doi.org/10.1016/j.polymdegradstab.2005.10.007, 2006.

Lazrus, A. L., Kok, G. L., Gitlin, S. N., Lind, J. A., and McLaren, S. E.: Automated fluorimetric method for hydrogen peroxide in atmospheric precipitation, Analytical Chemistry, 57, 917-922, https://doi.org/10.1021/ac00281a031, 1985.

Li, Q., Sritharathikhun, P., and Motomizu, S.: Development of novel reagent for Hantzsch reaction for the determination of formaldehyde by spectrophotometry and fluorometry, Analytical Sciences, 23, 413-417, https://doi.org/10.2116/analsci.23.413, 2007.

Vaïtilingom, M., Deguillaume, L., Vinatier, V., Sancelme, M., Amato, P., Chaumerliac, N., and Delort, A.-M.: Potential impact of microbial activity on the oxidant capacity and organic carbon budget in clouds, Proceedings of the National Academy of Sciences, 110, 559-564, 10.1073/pnas.1205743110, 2013.